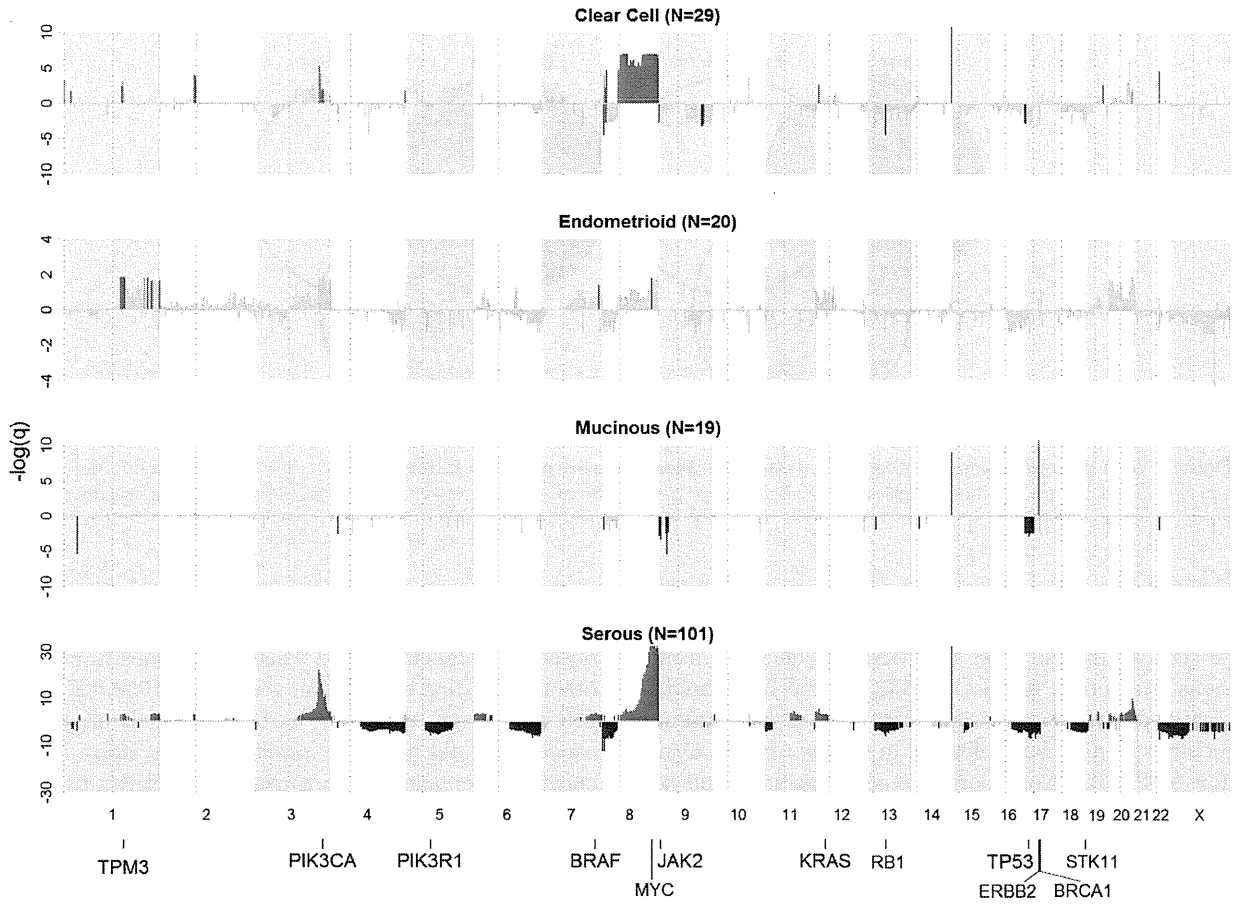

Figure 2 Significance of copy number alterations (green) in clear cell, endometrioid, mucinous, and serous histotypes are shown in 4 horizontal tracks respectively. GISTIC q-values (y-axis) are shown as $-\log_{10}$. Regions that passed the statistical selection criteria (see Methods) are shown as: amplification (red) and deletion (blue). Some known cancer and putative genes are indicated at the bottom of the plots. ERBB2 in chr17 is shown to be amplified in the mucinous track. Note scale difference in y-axis for the histotypes.

CNA are specific to histotypes, adding to the mounting evidence of molecular differences between histotypes. Despite larger sample size in serous histotype, comparison of CNA found in the lower prevalent histotypes with serous is also of interest (Additional file 3: Figure S2). Clear cell tumors had the highest number of common altered genes with serous tumors (7.6%) while endometrioid tumors had the lowest number of common altered genes; 3.0% common altered genes with serous tumors only. There is also more overlap on amplifications than deletions.

Consistency with other studies

Three studies have reported copy number changes in EOC [16,17,24] (Additional file 4: Table S2). These studies focused on global changes in EOC rather than histotype-specific alterations. Nevertheless, histotype-specific alterations from our study should overlap to some degree with these reported genes. We compiled a list of 551 significant genes reported in the 3 studies of which 545 genes were reported by either Haverty et al. or Gorringe et al. Eleven genes (2%) were commonly identified in at least 2 of the studies. In comparison, 39.2% (216/551) of genes were found in our study, indicating that our approach can identify copy number altered genes. We also compared our findings in serous tumors with TCGA high grade serous study (n=489) [23] where they reported 63 regions of gains and 50 regions of deletion. Based on overlapping of genes (if available) or genomic regions, 29/63 (46%) amplified and 27/50 (54%) deleted regions were also found in our study (n=101) (Additional file 5: Table S3).

Copy number alterations in known cancer genes

300 cancer genes were previously reported [25], of which 76 cancer genes were found within the altered regions (Table 1). We found that copy number alterations of these cancer genes were specific to histotypes as well;

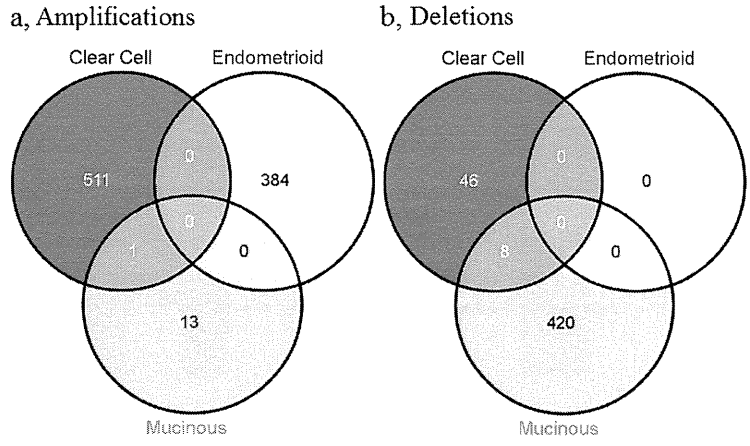

Figure 3 Venn diagram of copy number altered genes between the lower prevalent histotypes. Left: amplified genes; Right: deleted genes. Clear cell tumors had more amplified genes than deleted genes while mucinous tumors had more deleted genes than amplified genes.

e.g. TPM3 amplification in endometrioid tumors; JAK2 deletion in mucinous; RB1 deletion in both clear cell and serous tumors; TP53 and MAP2K4 deletion in mucinous and serous tumors. ERBB2, a gene implicated in breast and EOC showed significant focal amplification in mucinous tumors but deletions in serous tumors. Evaluation of ERBB2 expression between mucinous and serous tumors in the 3 datasets showed the trend of over expression of ERBB2 in mucinous compared to serous (Additional file 6: Table S4). The focal amplification of ERBB2 has been observed in various studies [26-28], supporting our findings.

Identification of candidate driver genes in EOC histotypes

To identify candidate driver genes that might contribute to carcinogenesis of EOC, we looked for genes that showed association between copy number and gene expression (Methods, Additional file 1: Figure S1). Table 1 summarized the alterations and potential cancer driver genes (highlighted in bold) based on cytoband. Pathway analysis of potential driver genes in Table 1 showed top molecular functions of these genes to be involved with cell cycle, cellular development, growth and proliferation.

Candidate drivers in known cancer genes

Among 76 identified cancer genes listed in Table 1, several genes were potential drivers (highlighted in bold) in EOC in the association analysis. These include: FH, GMPS, PIK3CA, EIF4A2, ZNF384, and SS18L1 (amplifications in serous tumors); TET2, FGFR10P, NF1, ERBB2, and SH3GL1 (deletions in serous tumors) and ERBB2 (amplifications in mucinous tumors). Figure 4 shows the association between copy number and gene expression of ERBB2. The correlation was significant for all 3 datasets (Dataset1: R=0.80, p=3.47E-09, Dataset2: R=0.74, p=9.44E-6, Dataset3: R=0.79, p=1.14E-6, meta-p=3.90E-17), suggesting a driver mechanism. Amplification was observed in mucinous and deletion in serous tumors. Another interesting observation was MYC, TP53, KRAS, and BRCA1, genes reportedly to be commonly mutated in cancers but did not show significant association between copy number and gene expression. Similarly, two other genes reported to be mutated in EOC (PIK3R1 and STK11) also did not show potential driver mechanism.

Validation of ERBB2 expression

It is not within the scope of this study to validate the candidate copy number driver genes. As ERBB2 has potential for targeted therapy, we validated the expressions of ERBB2 via qPCR of 7 samples in Dataset1 that were found to be amplified or deleted. It should be noted that no more samples were available in Dataset2 for validation. Figure 5 shows the scatter plot between gene expression from microarray and qPCR (measured as fold-change). Significant correlation was observed (p=0.007) between microarray and qPCR. Four ERBB2 amplified samples (1 serous, 1 mucinous, 1 mucinous borderline, and 1 clear cell) were expressed correspondingly higher than the 3 serous samples with deleted ERBB2 (p=0.06, Wilcoxon). All these data support ERBB2 as a copy number driver gene in EOC.

Discussion

The study reveals genomics diversity in EOC. It is conceivable that some of these alterations are involved in the tumorigenesis of EOC but the pathogenesis is likely regulated by aberrations of histotype specific alterations. By stratifying based on histotypes, we were able to identify alterations in the lower prevalent clear cell, endometrioid, and mucinous samples. An example is ERBB2.

Table 1 Summary of copy number alterations and potential driver cancer genes

Region	AMP				DEL				Cancer genes
	C	E	M	S	C	E	M	S	
1p36.11								D	MDS2
1q21.2-1q21.3		A							ARNT,**TPM3**
1q21.1-1q23.1		A		A					**BCL9**,MUC1,PRCC,NTRK1
1q42.13-1q44				A					**FH**
3q21.1-3q26.1				A					FOXL2,**GMPS**,MLF1
3q26.31-3q29				A					**PIK3CA**,ETV5,**EIF4A2**,BCL6,LPP,TFRC
4q21.22-4q31.3								D	RAP1GDS1,**TET2**,IL2,FBXW7
5q11.2-5q23.1								D	IL6ST,PIK3R1,APC
6p22.1-6p25.3				A					IRF4,DEK,HIST1H4I
6q22.2-6q27								D	ROS1,GOPC,STL,MYB,TNFAIP3,**FGFR1OP**,MLLT4
7q32.1-7q36.3				A					SMO,CREB3L2,KIAA1549,**BRAF**,EZH2
8p12-8p23.3								D	PCM1,WRN,WHSC1L1
8q11.21-8q24.3	A			A					HOOK3,**TCEA1**,CHCHD7,PLAG1,NCOA2,COX6C,EXT1,MYC,**RECQL4**
9p21.3-9p24.1							D		JAK2,MLLT3
11p15.4								D	CARS,NUP98,LMO1
11q13.3-11q21				A					**NUMA1**,PICALM,MAML2
12p11.21-12p13.33				A					KDM5A,CCND2,**ZNF384**,ETV6,KRAS
13q12.2-13q14.3								D	CDX2,FLT3,BRCA2,LHFP,LCP1
13q14.2					D			D	**RB1**
15q14-15q15.1								D	BUB1B
16q13-16q23.3								D	HERPUD1,CBFB,CDH1,MAF
17p11.2-17p13.2							D	D	USP6,TP53,PER1,GAS7,MAP2K4
17q11.1-17q21.31								D	**NF1**,SUZ12,TAF15,MLLT6,LASP1,RARA,BRCA1
17q12			A					D	**ERBB2**
18q21.32-18q22.2								D	MALT1,BCL2
19p13.3								D	FSTL3,STK11,TCF3,**SH3GL1**,MLLT1
20q11.21-20q13.33				A					ASXL1,GNAS,**SS18L1**
22q11.21-22q13.33								D	CLTCL1,MN1,CHEK2,EWSR1,NF2,MYH9,PDGFB,MKL1,MKL1,EP300
Xp11.3-Xp22.33								D	P2RY8,KDM6A
Xq25								D	ELF4

For simplicity, the altered regions are summarized into cytobands in the first column. Second (AMP) and third (DEL) columns indicate the amplification and deletion respectively for each histotype (C-clear cell, E-endometrioid, M-mucinous, S-serous). The amplification (A) and deletion (D) status for each histotype are indicated in each cytoband. The last column shows known cancer genes (from Sanger COSMIC database) that are within the altered regions. In total, 76 genes are listed in this table. Cancer genes which are potential drivers (i.e. significant correlation between gene expression and copy number alterations) are highlighted in bold.

Several groups have investigated alterations of ERBB2 in EOC with mixed results [29,30]. However, when stratified into histotypes, the high prevalence of ERBB2 amplification in mucinous is clearly evident in our results and other studies [26-28]. In addition, our results support ERBB2 as a potential copy number driver gene in EOC. The differences of ERBB2 copy number alterations amongst the histotypes could be due to the origin of histotypes in EOC. Our study demonstrates the importance of histotype-specific analyses where the differing copy number landscape amongst the histotypes adds to the mounting evidence that EOC should not be treated as one disease.

76 cancer genes listed in Table 1 were found to be copy number altered in EOC. They include ERBB2, TPM3, BRCA1, BRAF, KRAS, and PIK3CA; some of which are potential copy number drivers e.g. PIK3CA and BRAF in serous histotypes. Another interesting observation was KRAS, a gene reported to be mutated in mucinous tumors. In our study, KRAS was not found significantly altered in mucinous tumors where mutations are common. However, KRAS was significantly amplified in serous tumors where mutations are rare in high grade tumors. The reciprocal relationship between KRAS mutation and copy number alterations is also observed in gastric cancer [11]. The 8q24.21 region

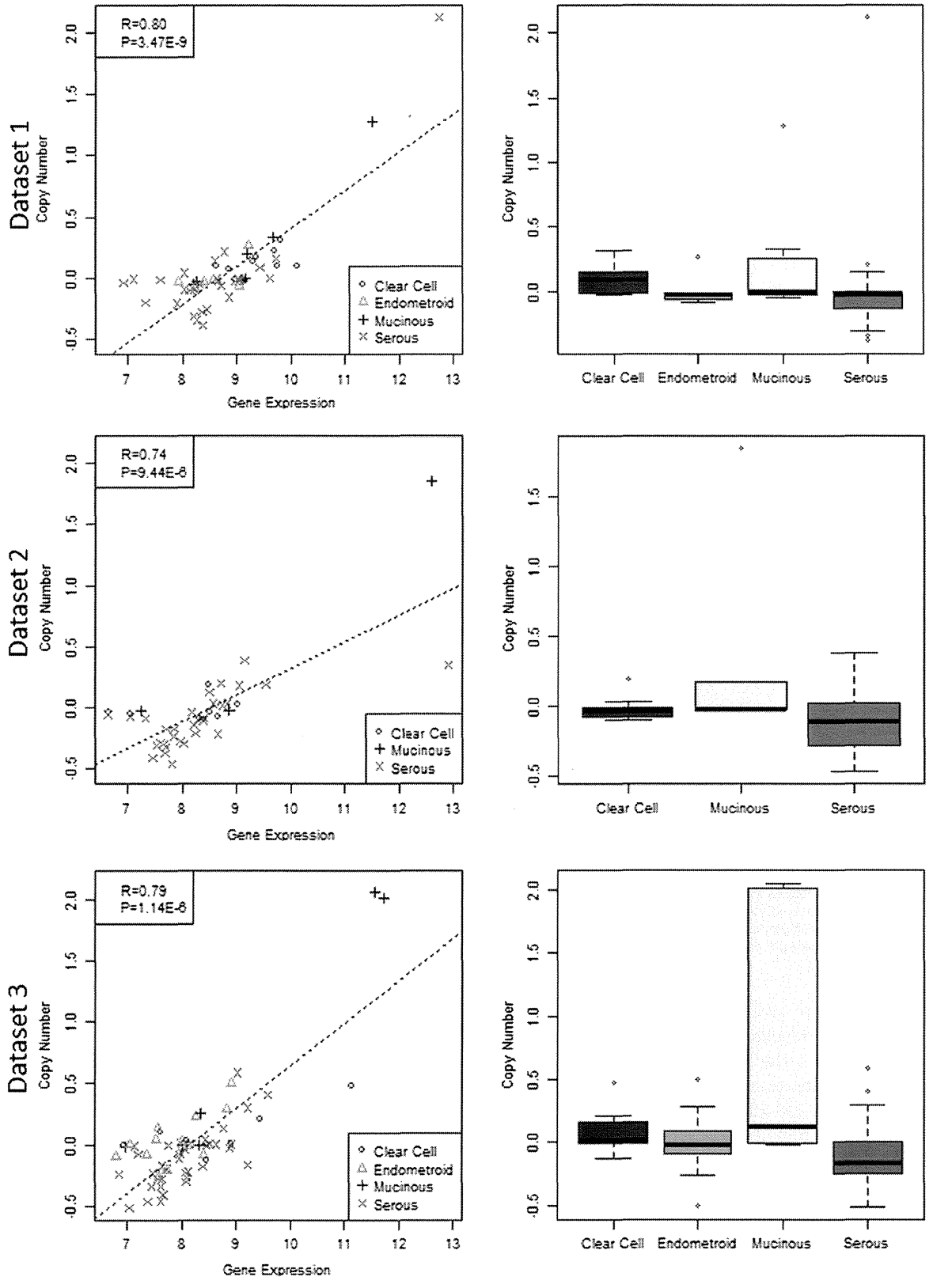

Figure 4 (See legend on next page.)

(See figure on previous page.)
Figure 4 Copy number and gene expression of ERBB2 for 3 datasets. From top: dataset1, dataset2, dataset3. Each row shows (left) the correlation between copy number and gene expression, and (right) boxplot of copy number across histotypes. Significant correlations were observed between gene expression and copy number alterations, suggesting a potential copy number driver mechanism.

harboring MYC, on the other hand, was altered in most histotypes other than mucinous. TCGA study also indicates MYC is highly amplified in high grade serous tumors. This suggests that MYC inhibitors may be applicable for these histotypes. For cancer genes which have been reported to have somatic or germline mutations in EOC, 3 were found to harbor copy deletions in serous histotype: PIK3R1, BRCA1, and STK11. For BRCA1, our finding was concordant with previous report that BRCA1 locus could be lost via either deletion or epigenetic silencing other than mutation in sporadic EOC [31].

A number of the candidate drivers in Table 1 are also implicated in translocation aberrations, e.g. TPM3, BCL9, GMPS, ZNF384 and SS18L1. It's interesting that these genes were amplified in endometrioid and/or serous tumors. TPM3 and BCL9 reside in 1q21, a frequent site for chromosomal rearrangements. TPM3 was specifically amplified in endometrioid tumors and the gene has been shown to constitute a fusion gene with NTRK1 which belongs to the group of TRK oncogenes reported for papillary thyroid carcinoma [32]. Interestingly, NTRK1 is also significantly amplified only in endometrioid tumors and further investigation is required to ascertain if this is due to gene fusion. BCL9 is a novel oncogene in Wnt signaling pathway, playing a critical role in epithelial-mesenchymal transition in colon epithelium and adenocarcinomas [33,34]. Translocation of BCL9 has been reported with 14q32 [35] and the gene was amplified in both endometrioid and serous tumors. Translocations for GMPS, ZNF384, and SS18L1 were also found in leukemia and synovial sarcomas [36-40] and all were amplified in serous tumors.

There are several drugs targeting the genes, e.g. for ERBB2, inhibitors include Trastuzumab, Lapatinib, and Pertuzumab. Lately, a clinical trial on combination of Pertuzumab, Trastuzumb and Docetaxel improved outcome of patients with HER2 positive metastatic breast cancer [41]. BRAF mutations are more common in low grade serous while BRAF amplification is more common in high grade serous. Our data showed that it is a potential copy number driver and hence may be targetable by BRAF-inhibitors in serous tumors. Most BRAF inhibitors target various mutations and its efficacy on amplified BRAF is not yet well understood. A study has shown that BRAF amplified colorectal cancer cells acquired resistance to the

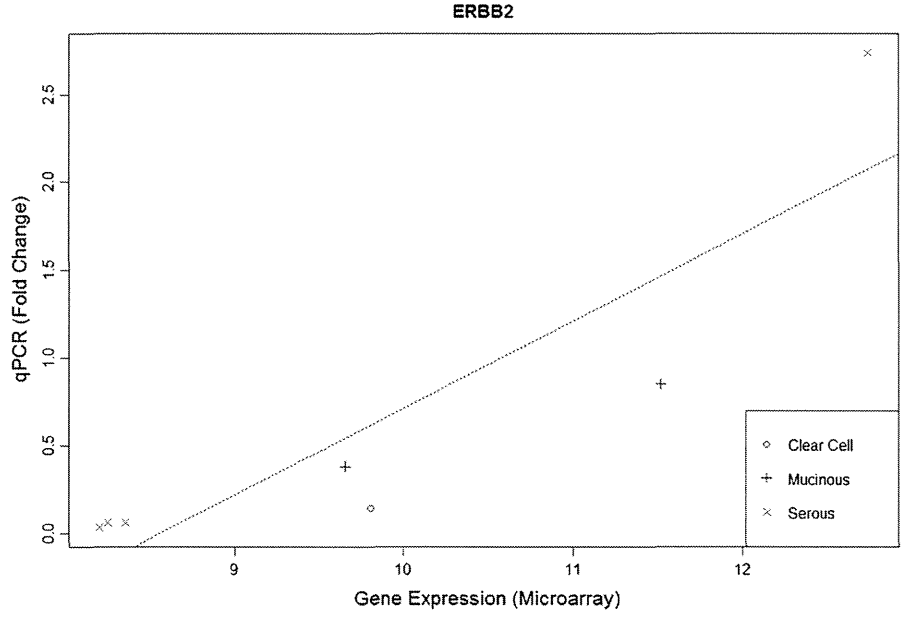

Figure 5 Scatter plot of ERBB2 gene expression and qPCR of 7 samples identified to be copy number altered in Dataset1. 4 ERBB2 amplified samples (serous, mucinous, mucinous borderline, and clear cell) had higher expression than the 3 ERBB2 deleted serous samples. Significant correlation was observed between gene expression and qPCR (p=0.007).

MEK1/2 inhibitors selumetinib [42]. PIK3CA is significantly amplified in serous histotypes and could be a potential target for PI3K inhibitors. In a study of PI3K inhibitor on breast and gynecologic malignancies harboring PIK3CA mutations, patients with the mutations treated with the inhibitor showed higher response rate than patients without the mutations [43].

In combining the 3 datasets, there was concern with regards to the genetic diversity amongst the Chinese Japanese, and Caucasian samples. The Hapmap [44] and Human Genome Diversity projects [45] have showed that these ethnic groups are different, though Chinese (CHB) and Japanese (JPT) tend to have high similarity in population structure. As genetic differences can be evaluated via principal component analysis (PCA) [46], we used PCA to assess the copy number data of the 3 cohorts. No distinct clustering between the groups (Additional file 7: Figure S3) was observed, suggesting that in this particular copy number landscape, the genetic effect is not evident and therefore has minimal effect in the analyses. We also used ANOVA test to assess ~200 housekeeping genes between the 3 datasets; none of the genes showed significance (Additional file 8: Table S5). Note that ERBB2 also did not show any significance. Nevertheless, genetic differences were taken into consideration in the preprocessing protocol. Individual dataset was normalized with respect to the relevant ethnic group from Hapmap data, i.e. Dataset1 with JPT, and Dataset2 with CHB. Ethnic-specific common structural polymorphism was also filtered out (see Data analysis) to ensure the copy number alterations identified in this study are de novo alterations in tumors.

We recognize that the regions identified could still be limited by the individual sample size of the histotypes. The larger number of copy number altered genes in serous tumors could be attributed to the larger sample size in this collection. We performed sub-sampling analyses to ascertain the effects and in addition, to ensure robustness of results, we used stringent criteria to filter the regions as well as criteria to consider CNA genes if it were supported by at least 2 dataset (Additional file 1: Figure S1). The flip side of this filtering was that true regions of alterations could be filtered out (as shown in the green area in Figure 1), leading to probably more false negatives. Nevertheless, we observed that despite the filtering and limited sample size of some histotypes, significant regions were still observed in the less prevalent histotypes; e.g. the 1p36.33, 2p11.1, 19q13.31, and 20q13.33 amplification and 9q32 deletion in clear cell tumors (n=29); 1q21.2-3 amplification in endometrioid tumors (n=20); 17q12 amplification and p24.1 deletion in mucinous tumors (n=19). Note that endometrioid tumors were not available in Dataset 2 although the total number of tumors was comparable with clear cell and mucinous. The concordance criteria of agreement on 2 datasets in the analytical workflow would thus bias the identification of regions for this histotype. Despite this, significant alterations were still observed for endometroid (e.g. TPM3) and given the stringent criteria; these are likely high confidence alterations. It should be noted that the samples were stratified according to the 4 main histotypes, including some borderline cases. Although borderline cases are presented clinically as a different subtype, they were included to simplify the stratification of histotypes and analyses. The significance of this approach can be seen in ERBB2, where both mucinous and mucinous borderline cases harbor amplification and corresponding up regulation of expression as well. This was similarly observed in other studies [26-28]. To assess if copy number alterations differ between borderline and non-borderline tumors and would thus cause bias in our analyses, we evaluated PCA of these samples (Additional file 9: Figure S4). No distinct clustering was observed between the borderline and non-borderline groups.

Conclusions

In summary, our study showed genomic diversity in EOC and highlighted distinct copy number alterations in histotypes that may have potential for drug targeted therapy. ERBB2 is significantly amplified in mucinous tumors and is a candidate copy number driver gene. By merging multiple datasets of similar platform, we demonstrated that CNA in the lower prevalent histotypes could be elucidated, even with limited sample size.

Methods

Dataset1

56 archived frozen tumor samples from the Department of Gynecology & Obstetrics, Kyoto University Graduate School of Medicine, Japan were profiled on microarray. It contained 12 clear cell carcinoma, 6 endometrioid adenocarcinoma, 2 mucinous adenocarcinoma, 5 mucinous-borderline tumors, 26 serous adenocarcinoma, and 5 serous-borderline tumors.

Dataset2

46 archived frozen tumor samples collected from Department of Obstetrics and Gynecology, Tri-Service General Hospital, Taiwan, containing 9 clear cell, 6 mucinous, and 31 serous.

Dataset3

GSE19539 consisting of 8 clear cell, 14 endometrioid, 6 mucinous, and 39 serous [15]. Blood normal available in the dataset was used for normalization in concordance with the paper.

Human ovarian carcinoma samples

Two collections of archived flash frozen ovarian carcinoma samples were obtained from the Department of Gynecology & Obstetrics, Kyoto University Graduate School of Medicine, Japan (Dataset1, N= 56) and Department of Obstetrics and Gynecology, Tri-Service General Hospital, Taiwan (Dataset2, N=46). All samples were collected with the donor's written informed consent. Ethical clearance has been approved by the Institutional Review Board for both institutes. All samples were reviewed by at least one pathologist from the respective institutes on histopathological typing and purity of samples. Tumor genomic DNAs were extracted by using phenol-chloroform extraction method. Tumor RNAs were extracted by using Qiazol followed by column clean-up using miRNeasy kit (Qiagen).

Copy number profiling

Affymetrix Genome-Wide Human SNP Arrays 6.0 (Affymetrix, Santa Clara, California) were used for copy number analysis according to the cytogenetics protocol from the manufacturer. Data was pre-processed and normalized with Hapmap JPT or CHB for Japan and Taiwan samples respectively using the Affymetric Genotyping Console. Copy number segments were obtained from the circular binary segmentation (CBS) algorithm [47] implemented in R package DNAcopy using default settings.

Gene expression profiling

Affymetrix GeneChip Human Gene 1.0ST Array was used for gene expression analysis according to the protocols from the manufacturer. Data was pre-processed and RMA normalized [48] using Affymetrix Gene Expression Console. Expressions for genes were mean-aggregated for each gene based on Affymetrix probes annotation. Note: 3 mucinous samples in Dataset2 and 2 serous samples in Dataset3 do not have corresponding gene expression data.

Data repository

The gene expression and copy number datasets are MIAME compliant and have been submitted to National Centre for Biotechnology Information's (NCBI) Gene Expression Omnibus (GEO) website, series accession number GSE30311.

Quantitative real time PCR

Total and miRNA was isolated from the ovarian carcinoma tissues using the miRNeasy kit (QIAGEN), of which 500ng were used to generate cDNA using the RT^2 first strand kit (QIAGEN). For the qPCR run, 200ng of first strand cDNA was used per gene analysis. To determine the expression profile, ERBB2 transcript expression levels were normalized against the averaged expression levels of 5 housekeeping genes (ACTB, B2M, GADPH, HPRT and RPL13A).

Delta-C_t (ΔC_t) and fold-change determination

C_t was determined using the SDS software (version 2.3, Applied Biosystems). Briefly, C_t values were determined by setting the baseline between cycle 2 of the run (total run: 40 cycles) and 2 cycles before the start of the first log-phase amplification. The threshold was set by positioning the limit to the lower third of the earliest amplification. ΔC_t was calculated by the formulae:

$$\Delta C_t = C_t(\mathrm{GOI}) - C_t(\mathrm{HKG})$$

whereby: C_t (GOI): C_t value of the respective gene of interest (GOI), C_t (HKG): average C_t values of the 5 housekeeping genes (HKG) used in the assay, Fold-change of the transcript is determined by the following formula:

$$\mathrm{Fold-change} = 2^{(-\Delta Ct)}$$

Data analysis

To identify significant copy number altered regions, we used a 2-pronged workflow employing the GISTIC algorithm [18]. GISTIC identifies copy number alterations based on the frequency as well as the log relative ratio (LRR) signals to compute the q value (false discovery rate). Default settings were used in the GISTIC analysis, and amplification and deletion thresholds were set at 0.2 and −0.2 respectively. Additional file 1: Figure S1 shows the 2-pronged workflow involving merged and individual copy number datasets to identify copy number alterations. Alterations were considered significant if it passed the following filtering criteria: (i) $q < 0.25$ (individual dataset), (ii) $q < 0.05$ (merged dataset), and (iii) concordance in 2 or more datasets. The significant regions were than mapped to genes (hg18 Refseq) by averaging the segments within each gene. ANOVA test was used to identify histotype-specific alterations. The analyses resulted in a list of significant gain and loss genes for each histotype, summarized in Figure 2 and Table 1 (known cancer genes).

To identify potential driver genes, non-parametric Spearman correlation was used to assess association between gene expression and copy number alterations of individual gene for each dataset (Additional file 1: Figure S1). Fisher's combined probability test (meta-p) [49] was then used to combine the correlation statistics from each dataset to identify potential driver genes. This hypothesis driven association approach has been used to identify potential cancer driver genes [50,51]. Potential driver genes of known cancer genes are listed in Table 1 (in bold).

PCA plots were generated using Partek Genomics Suite (Partek, Missouri, USA). Pathway analyses were performed using Ingenuity Pathway Analysis software

(Ingenuity, California, USA). The frequency plot for copy number altered regions in Figure 1 was generated using the threshold of LRR ≥ |0.2|. All statistical analyses and plots were done using the R programming package (http://www.r-project.org).

Sub-sampling analyses to ascertain effects of sample size

To assess the effects of disparate sample size of the histotypes in the merged copy number data, multiple sub-sampling (with replacement) on the merged serous tumors was performed to ascertain the false positive and negative. The results showed that ≥97% of genes identified in sample size of 20–30 were also found in sample size of 101. However, 43-57% of genes found in the larger sample size were not identified in the smaller sample size datasets. In view of this, we have mainly confined comparison of genes found in the non-serous tumors.

Additional files

Additional file 1: Figure S1. Data Analysis Workflow. Two pronged approach for individual and merged datasets through selective threshold of GISTIC q-value and concordance in copy number analysis. As some histotypes have lower prevalence, filtering thresholds for individual and merged dataset were set at q<0.25 and q<0.05 respectively to overcome differences in sample size. In addition, any genomic alterations are supported by at least 2 datasets (i.e. concordance criteria). Specifically, the filtering criteria for histotype-specific regions were: (i) $q < 0.25$ (individual dataset), (ii) $q < 0.05$ (merged dataset), and (iii) concordance in 2 or more datasets. This resulted in a list of significant gains and loss regions. To identify copy number driver genes that are specific to histotype, copy number segments were mapped to genes and ANOVA was used to identify the differentially altered genes. This resulted in a list of histotype-specific altered genes. Spearman correlation between gene expression and copy number was then used to assess potential driver genes in each individual dataset.

Additional file 2: Table S1. Summary of overlapped amplified and deleted genes between histotypes.

Additional file 3: Figure S2. Venn diagram of copy number altered genes between the 4 histotypes. Left: amplified genes; Right: deleted genes. Clear cell tumors had the highest number of common altered genes with serous tumors while endometrioid tumors had the lowest number of common altered genes.

Additional file 4: Table S2. Summary of datasets used for comparison of commonly altered genes.

Additional file 5: Table S3. Summary of comparison with TCGA.

Additional file 6: Table S4. Comparison of ERBB2 expression between mucinous and serous tumors.

Additional file 7: Figure S3. Principal component analysis of copy number altered gene from the merged datasets. The plot shows that there is minimal copy number alterations difference between the 3 datasets.

Additional file 8: Table S5. Summary of anova results on the 3 datasets.

Additional file 9: Figure S4. Principal component analysis of copy number altered genes from the merged datasets showing borderline and non-borderline tumors. Borderline tumors were available only in serous and mucinous histotypes. No distinct clustering was observed between borderline and non-borderline tumors for (a) mucinous and (b) serous.

Abbreviations

EOC: Epithelial ovarian cancer; PCR: Polymerase chain reaction; qPCR: Quantitative real-time polymerase chain reaction; FDR: False discovery rate; TCGA: The cancer genome atlas; PCA: Principal component analysis; CHB: Hapmap Chinese; JPT: Hapmap Japanese; CBS: Circular binary segmentation; NCBI: National Centre for Biotechnology Information; GEO: Gene expression omnibus; GOI: Gene of interest; HKG: Housekeeping genes; GISTIC: Genomic identification of significant targets in cancer; ANOVA: Analysis of variance.

Competing interests

The authors declare no competing interests.

Authors' contributions

RYJH, JPT, and LG drafted the manuscript. GBC and LG performed the analyses. NM, HCL, IK collected the tissues. RYJH, SM, MKW extracted the RNA and DNA for profiling. RYJH and MKW carried out the PCR. LG conceived of the study. All authors read and approved the final manuscript.

Acknowledgements

We thank Duke-NUS Genome Biology Facility for their help in profiling the samples in Dataset1. This study is supported by Khoo Discovery Award KDP/2008/0002 and KDP/2009/0006, and Duke-NUS core grant (LG), and National Research Foundation (RYH, JPT). We like to thank the reviewers for their constructive comments which have greatly improved the manuscript.

Author details

[1]Department of Obstetrics & Gynaecology, National University Hospital, 5 Lower Kent Ridge Road, Singapore 119074, Singapore. [2]Cancer Science Institute, National University of Singapore, Centre for Life Sciences, #02-07 28 Medical Drive, Singapore 117456, Singapore. [3]Cancer & Stem Cell Biology, Duke-National University of Singapore Graduate Medical School, 8 College road, Rm 6-32, Singapore 169857, Singapore. [4]Department of Gynecology and Obstetrics, Kyoto University Graduate Medical School, Yoshida-Konoe-cho, Sakyo-ku, Kyoto 606-8501, Japan. [5]National Defense Medical Center, Taiwan, 114 No.161, Sec. 6, Minquan E. Rd., Neihu Dist, Taipei City 114, Taiwan. [6]Institute of Molecular and Cell Biology, 61 Biopolis Drive, Proteos, Singapore 138673, Singapore. [7]Department of Medical Oncology, National Cancer Centre Singapore, 11 Hospital Drive, Singapore 169610, Singapore. [8]Saw Swee Hock School of Public Health, Yong Loo Lin School of Medicine, National University of Singapore, MD3, 16 Medical Drive, Singapore 117597, Singapore.

Received: 14 March 2012 Accepted: 11 October 2012
Published: 18 October 2012

References

1. Sankaranarayanan R, Ferlay J: **Worldwide burden of gynaecological cancer: the size of the problem.** *Best Pract Res Clin Obstet Gynaecol* 2006, **20**(2):207–225.
2. Bonome T, Levine DA, Shih J, Randonovich M, Pise-Masison CA, Bogomolniy F, Ozbun L, Brady J, Barrett JC, Boyd J, *et al*: **A gene signature predicting for survival in suboptimally debulked patients with ovarian cancer.** *Cancer Res* 2008, **68**(13):5478–5486.
3. Jemal A, Siegel R, Ward E, Murray T, Xu J, Smigal C, Thun MJ: **Cancer statistics, 2006.** *CA Cancer J Clin* 2006, **56**(2):106–130.
4. Chuaqui RF, Cole KA, Emmert-Buck MR, Merino MJ: **Histopathology and molecular biology of ovarian epithelial tumors.** *Ann Diagn Pathol* 1998, **2**(3):195–207.
5. Khalil I, Brewer MA, Neyarapally T, Runowicz CD: **The potential of biologic network models in understanding the etiopathogenesis of ovarian cancer.** *Gynecol Oncol*, **116**(2):282–285.
6. Sieben NL, Macropoulos P, Roemen GM, Kolkman-Uljee SM, Jan Fleuren G, Houmadi R, Diss T, Warren B, Al Adnani M, De Goeij AP, *et al*: **In ovarian neoplasms, BRAF, but not KRAS, mutations are restricted to low-grade serous tumours.** *J Pathol* 2004, **202**(3):336–340.
7. Ahmed AA, Etemadmoghadam D, Temple J, Lynch AG, Riad M, Sharma R, Stewart C, Fereday S, Caldas C, Defazio A, *et al*: **Driver mutations in TP53 are ubiquitous in high grade serous carcinoma of the ovary.** *J Pathol* 2010, **221**(1):49–56.
8. Enomoto T, Weghorst CM, Inoue M, Tanizawa O, Rice JM: **K-ras activation occurs frequently in mucinous adenocarcinomas and rarely in other common epithelial tumors of the human ovary.** *Am J Pathol* 1991, **139**(4):777–785.

9. Obata K, Morland SJ, Watson RH, Hitchcock A, Chenevix-Trench G, Thomas EJ, Campbell IG: **Frequent PTEN/MMAC mutations in endometrioid but not serous or mucinous epithelial ovarian tumors.** *Cancer Res* 1998, **58**(10):2095–2097.
10. Stratton MR, Campbell PJ, Futreal PA: **The cancer genome.** *Nature* 2009, **458**(7239):719–724.
11. Deng N, Goh LK, Wang H, Das K, Tao J, Tan IB, Zhang S, Lee M, Wu J, Lim KH, *et al*: **A comprehensive survey of genomic alterations in gastric cancer reveals systematic patterns of molecular exclusivity and co-occurrence among distinct therapeutic targets.** *Gut* 2012, **61**(5):673–684.
12. Janku F, Stewart DJ, Kurzrock R: **Targeted therapy in non-small-cell lung cancer–is it becoming a reality?** *Nat Rev Clin Oncol* 2010, **7**(7):401–414.
13. Barnes DJ, Melo JV: **Management of chronic myeloid leukemia: targets for molecular therapy.** *Semin Hematol* 2003, **40**(1):34–49.
14. Verma S, Lavasani S, Mackey J, Pritchard K, Clemons M, Dent S, Latreille J, Lemieux J, Provencher L, Verma S, *et al*: **Optimizing the management of her2-positive early breast cancer: the clinical reality.** *Curr Oncol* 2010, **17**(4):20–33.
15. Ramakrishna M, Williams LH, Boyle SE, Bearfoot JL, Sridhar A, Speed TP, Gorringe KL, Campbell IG: **Identification of candidate growth promoting genes in ovarian cancer through integrated copy number and expression analysis.** *PLoS One* 2010, **5**(4):e9983.
16. Gorringe KL, Ramakrishna M, Williams LH, Sridhar A, Boyle SE, Bearfoot JL, Li J, Anglesio MS, Campbell IG: **Are there any more ovarian tumor suppressor genes? A new perspective using ultra high-resolution copy number and loss of heterozygosity analysis.** *Genes Chromosomes Cancer* 2009, **48**(10):931–942.
17. Haverty PM, Hon LS, Kaminker JS, Chant J, Zhang Z: **High-resolution analysis of copy number alterations and associated expression changes in ovarian tumors.** *BMC Med Genomics* 2009, **2**:21.
18. Beroukhim R, Getz G, Nghiemphu L, Barretina J, Hsueh T, Linhart D, Vivanco I, Lee JC, Huang JH, Alexander S, *et al*: **Assessing the significance of chromosomal aberrations in cancer: methodology and application to glioma.** *Proc Natl Acad Sci USA* 2007, **104**(50):20007–20012.
19. Rodabaugh KJ, Biggs RB, Qureshi JA, Barrett AJ, Welch WR, Bell DA, Berkowitz RS, Mok SC: **Detailed deletion mapping of chromosome 9p and p16 gene alterations in human borderline and invasive epithelial ovarian tumors.** *Oncogene* 1995, **11**(7):1249–1254.
20. Feltmate CM, Lee KR, Johnson M, Schorge JO, Wong KK, Hao K, Welch WR, Bell DA, Berkowitz RS, Mok SC: **Whole-genome allelotyping identified distinct loss-of-heterozygosity patterns in mucinous ovarian and appendiceal carcinomas.** *Clin Cancer Res* 2005, **11**(21):7651–7657.
21. Campbell IG, Foulkes WD, Beynon G, Davis M, Englefield P: **LOH and mutation analysis of CDKN2 in primary human ovarian cancers.** *Int J Cancer* 1995, **63**(2):222–225.
22. Devlin J, Elder PA, Gabra H, Steel CM, Knowles MA: **High frequency of chromosome 9 deletion in ovarian cancer: evidence for three tumour-suppressor loci.** *Br J Cancer* 1996, **73**(4):420–423.
23. Cancer Genome Atlas Research Network: **Integrated genomic analyses of ovarian carcinoma.** *Nature* 2011, **474**(7353):609–615.
24. Gorringe KL, Jacobs S, Thompson ER, Sridhar A, Qiu W, Choong DY, Campbell IG: **High-resolution single nucleotide polymorphism array analysis of epithelial ovarian cancer reveals numerous microdeletions and amplifications.** *Clin Cancer Res* 2007, **13**(16):4731–4739.
25. Futreal PA, Coin L, Marshall M, Down T, Hubbard T, Wooster R, Rahman N, Stratton MR: **A census of human cancer genes.** *Nat Rev Cancer* 2004, **4**(3):177–183.
26. Yan B, Choo SN, Mulyadi P, Srivastava S, Ong CW, Yong KJ, Putti T, Salto-Tellez M, Lim GS: **Dual-colour HER2/chromosome 17 chromogenic in situ hybridisation enables accurate assessment of HER2 genomic status in ovarian tumours.** *J Clin Pathol* 2011, **64**(12):1097–1101.
27. McAlpine JN, Wiegand KC, Vang R, Ronnett BM, Adamiak A, Kobel M, Kalloger SE, Swenerton KD, Huntsman DG, Gilks CB, *et al*: **HER2 overexpression and amplification is present in a subset of ovarian mucinous carcinomas and can be targeted with trastuzumab therapy.** *BMC Cancer* 2009, **9**:433.
28. Han CP, Hsu JD, Yao CC, Lee MY, Ruan A, Tyan YS, Yang SF, Chiang H: **HER2 gene amplification in primary mucinous ovarian cancer: a potential therapeutic target.** *Histopathology* 2010, **57**(5):763–764.
29. Nakayama K, Nakayama N, Jinawath N, Salani R, Kurman RJ, Shih Ie M, Wang TL: **Amplicon profiles in ovarian serous carcinomas.** *Int J Cancer* 2007, **120**(12):2613–2617.
30. Pastor T, Popovic B, Gvozdenovic A, Boro A, Petrovic B, Novakovic I, Puzovic D, Lukovic L, Milasin J: **Alterations of c-Myc and c-erbB-2 genes in ovarian tumours.** *Srp Arh Celok Lek* 2009, **137**(1–2):47–51.
31. Senturk E, Cohen S, Dottino PR, Martignetti JA: **A critical re-appraisal of BRCA1 methylation studies in ovarian cancer.** *Gynecol Oncol* 2010, **119**(2):376–383.
32. Greco A, Miranda C, Pierotti MA: **Rearrangements of NTRK1 gene in papillary thyroid carcinoma.** *Mol Cell Endocrinol* 2010, **321**(1):44–49.
33. Deka J, Wiedemann N, Anderle P, Murphy-Seiler F, Bultinck J, Eyckerman S, Stehle JC, Andre S, Vilain N, Zilian O, *et al*: **Bcl9/Bcl9l are critical for Wnt-mediated regulation of stem cell traits in colon epithelium and adenocarcinomas.** *Cancer Res* 2010, **70**(16):6619–6628.
34. Mani M, Carrasco DE, Zhang Y, Takada K, Gatt ME, Dutta-Simmons J, Ikeda H, Diaz-Griffero F, Pena-Cruz V, Bertagnolli M, *et al*: **BCL9 promotes tumor progression by conferring enhanced proliferative, metastatic, and angiogenic properties to cancer cells.** *Cancer Res* 2009, **69**(19):7577–7586.
35. Huret JL, Senon S, Bernheim A, Dessen P: **An Atlas on genes and chromosomes in oncology and haematology.** *Cell Mol Biol (Noisy-le-Grand)* 2004, **50**(7):805–807.
36. Storlazzi CT, Mertens F, Mandahl N, Gisselsson D, Isaksson M, Gustafson P, Domanski HA, Panagopoulos I: **A novel fusion gene, SS18L1/SSX1, in synovial sarcoma.** *Genes Chromosomes Cancer* 2003, **37**(2):195–200.
37. Martini A, La Starza R, Janssen H, Bilhou-Nabera C, Corveleyn A, Somers R, Aventin A, Foa R, Hagemeijer A, Mecucci C, *et al*: **Recurrent rearrangement of the Ewing's sarcoma gene, EWSR1, or its homologue, TAF15, with the transcription factor CIZ/NMP4 in acute leukemia.** *Cancer Res* 2002, **62**(19):5408–5412.
38. La Starza R, Aventin A, Crescenzi B, Gorello P, Specchia G, Cuneo A, Angioni A, Bilhou-Nabera C, Boque C, Foa R, *et al*: **CIZ gene rearrangements in acute leukemia: report of a diagnostic FISH assay and clinical features of nine patients.** *Leukemia* 2005, **19**(9):1696–1699.
39. Zhong CH, Prima V, Liang X, Frye C, McGavran L, Meltesen L, Wei Q, Boomer T, Varella-Garcia M, Gump J, *et al*: **E2A-ZNF384 and NOL1-E2A fusion created by a cryptic t(12;19)(p13.3; p13.3) in acute leukemia.** *Leukemia* 2008, **22**(4):723–729.
40. Pegram LD, Megonigal MD, Lange BJ, Nowell PC, Rowley JD, Rappaport EF, Felix CA: **t(3;11) translocation in treatment-related acute myeloid leukemia fuses MLL with the GMPS (GUANOSINE 5' MONOPHOSPHATE SYNTHETASE) gene.** *Blood* 2000, **96**(13):4360–4362.
41. Baselga J, Cortes J, Kim SB, Im SA, Hegg R, Im YH, Roman L, Pedrini JL, Pienkowski T, Knott A, *et al*: **Pertuzumab plus trastuzumab plus docetaxel for metastatic breast cancer.** *N Engl J Med* 2012, **366**(2):109–119.
42. Little AS, Balmanno K, Sale MJ, Newman S, Dry JR, Hampson M, Edwards PA, Smith PD, Cook SJ: **Amplification of the driving oncogene, KRAS or BRAF, underpins acquired resistance to MEK1/2 inhibitors in colorectal cancer cells.** *Sci Signal* 2011, **4**(166):ra17.
43. Janku F, Tsimberidou AM, Garrido-Laguna I, Wang X, Luthra R, Hong DS, Naing A, Falchook GS, Moroney JW, Piha-Paul SA, *et al*: **PIK3CA mutations in patients with advanced cancers treated with PI3K/AKT/mTOR axis inhibitors.** *Mol Cancer Ther* 2011, **10**(3):558–565.
44. International HapMap Consortium: **The International HapMap Project.** *Nature* 2003, **426**(6968):789–796.
45. Jakobsson M, Scholz SW, Scheet P, Gibbs JR, VanLiere JM, Fung HC, Szpiech ZA, Degnan JH, Wang K, Guerreiro R, *et al*: **Genotype, haplotype and copy-number variation in worldwide human populations.** *Nature* 2008, **451**(7181):998–1003.
46. Price AL, Patterson NJ, Plenge RM, Weinblatt ME, Shadick NA, Reich D: **Principal components analysis corrects for stratification in genome-wide association studies.** *Nat Genet* 2006, **38**(8):904–909.
47. Olshen AB, Venkatraman ES, Lucito R, Wigler M: **Circular binary segmentation for the analysis of array-based DNA copy number data.** *Biostatistics* 2004, **5**(4):557–572.
48. Irizarry RA, Bolstad BM, Collin F, Cope LM, Hobbs B, Speed TP: **Summaries of Affymetrix GeneChip probe level data.** *Nucleic Acids Res* 2003, **31**(4):e15.
49. Fisher RA: *Statistical methods for research workers*. Edinburgh: Oliver and Boyd; 1925.

50. Woo HG, Park ES, Lee JS, Lee YH, Ishikawa T, Kim YJ, Thorgeirsson SS: **Identification of potential driver genes in human liver carcinoma by genomewide screening.** *Cancer Res* 2009, **69**(9):4059–4066.
51. Lando M, Holden M, Bergersen LC, Svendsrud DH, Stokke T, Sundfor K, Glad IK, Kristensen GB, Lyng H: **Gene dosage, expression, and ontology analysis identifies driver genes in the carcinogenesis and chemoradioresistance of cervical cancer.** *PLoS Genet* 2009, **5**(11):e1000719.

doi:10.1186/1755-8794-5-47
Cite this article as: Huang *et al.*: Histotype-specific copy-number alterations in ovarian cancer. *BMC Medical Genomics* 2012 **5**:47.

JJCO Japanese Journal of Clinical Oncology

Clinical Trial Note

Jpn J Clin Oncol 2012;42(3)222–225
doi:10.1093/jjco/hyr201
Advance Access Publication 9 February 2012

Phase II Study of Oral Etoposide and Intravenous Irinotecan for Patients with Platinum-resistant and Taxane-pretreated Ovarian Cancer: Japan Clinical Oncology Group Study 0503

Koji Matsumoto[1,*], Noriyuki Katsumata[2], Isamu Saito[2], Taro Shibata[2], Ikuo Konishi[3], Haruhiko Fukuda[2] and Toshiharu Kamura[4]

[1]Hyogo Cancer Center, Kitaoji-cho, Akashi, Hyogo, [2]National Cancer Center, Tsukiji, Chuo-ku, Tokyo, [3]Kyoto University, Shogoinkawara-cho, Kyoto and [4]Kurume University, Asahi-cho, Kurume, Fukuoka, Japan

*For reprints and all correspondence: Koji Matsumoto, 13-70, Kitaoji-cho, Akashi, Hyogo, Japan.
E-mail: kojmatsu@hp.pref.hyogo.jp

Received September 24, 2011; accepted December 26, 2011

A single-arm Phase II study evaluating combination chemotherapy utilizing oral etoposide and irinotecan for platinum-resistant and taxane-pretreated ovarian cancer has started. The aim of this study is to evaluate the efficacy and safety of this regimen as a test arm regimen in a subsequent Phase III trial. Patients with platinum-resistant and taxane-pretreated ovarian cancer are given etoposide at 50 mg/m^2 p.o. from days 1 to 21 and irinotecan 70 mg/m^2 i.v. at days 1 and 15, repeated every 28 days, up to six cycles. A total of 60 patients will be enrolled at 36 institutions. The primary endpoint is response rate. The secondary endpoints include adverse events and progression-free and overall survival.

Key words: Chemo-Gynecology – Gynecol-Med – clinical trials

INTRODUCTION

Ovarian cancer is one of the most lethal gynecologic cancers in Japan. The first-line standard chemotherapy regimen is carboplatin plus paclitaxel (1,2). Although first-line chemotherapy is very effective, more than 60% of the patients with an advanced stage will die of recurrent disease. After relapse, the choice of second line chemotherapy depends on 'platinum-free interval (PFI)', which is prognostic and predictive for the effect of repeating platinum agents. Usually, the cut-off point of PFI is regarded as 6 months. Patients recurred within 6 months after first-line chemotherapy are regarded as 'platinum-resistant' and receive second-line chemotherapy with single agent such as pegylated liposomal doxorubicin (3), topotecan (3) and gemcitabine (4) as the standard treatment. Many single cytotoxic agents have shown activity against recurrent ovarian cancer; however, response rates generally have been low, such as 6–12% (3,4), and of short duration because of emerging resistance to the monotherapy regimens. Combination chemotherapy may circumvent this resistance and halt progression of disease, because lower dose of two drugs with different mechanism may reduce the toxicity and enhance the efficacy (5).

Irinotecan, a semi-synthetic derivative of camptothecin, is a prodrug with little inherent topoisomerase inhibitory activity and is converted by carboxylesterases to its more active metabolite, SN-38 (7-ethyl-10-hydroxycamptothecin). *In vitro*, SN-38 is 250–1000 times more potent than irinotecan as an inhibitor of topoisomerase. For platinum-resistant patients, irinotecan has shown modest activity (6–8) as monotherapy in weekly, every 2-week and every 3-week schedules.

Etoposide is a semi-synthetic glycosidic derivative of podophyllotoxin (9). Intravenous dosing of etoposide has been tested in two Phase II studies and shown relatively low response rates (10,11) (0 and 8.3%). On the contrary, oral etoposide has shown better efficacy, whose response rate was 26.8% for patients with platinum-resistant relapse (12).

Topoisomerase-I treatment induces an increase in the S-phase cell population with an increase in topoisomerase-II mRNA expression. Thus, topoisomerase-I can modulate topoisomerase-II levels to enhance the effect of topoisomerase-II inhibitors (13,14).

Eder et al. (15) reported the result of the *in vivo* study. They showed that a combination of irinotecan and etoposide showed more than an additive effect by both the tumor excision assay and tumor growth delay assay.

A Phase I study of topotecan and oral etoposide revealed severe myelosuppression but promising efficacy for ovarian cancer (16).

The dose-limiting toxicity of irinotecan is diarrhea, different from that of topotecan (myelosuppression). Then, utilizing etoposide with irinotecan may improve the risk–benefit balance of dual inhibition of topoisomerase. The result of the Phase I study was reported in ASCO 2002 (17).

The recommended dose for further study was oral etoposide: 50 mg/m^2/days 1–21 and intravenous irinotecan: 60 mg/m^2/days 1 and 15, repeated every 4 weeks.

In this Phase I study, four objective responses [two complete responses and two partial responses (PRs)] were achieved among 24 patients, including one PR in clear cell.

Nishio et al. (18) reported the result of feasibility study run by selected hospitals in Tohoku and Kyushu districts in Japan. Response rate, time to progression and overall survival were 44%, 9 months and 17 months, respectively.

This very promising result lead us to conduct a nationwide Phase II study run by Japan Clinical Oncology Group (JCOG).

The protocol review committee of the JCOG approved this protocol in January 2009 and the study was initiated in April 2009. This trial was registered at UMIN-CTR as UMIN000001837 (http://www.umin.ac.jp/ctr/index.htm).

PROTOCOL DIGEST OF THE JCOG0503

Objectives

The aim of this study is to evaluate the safety and efficacy of oral etoposide and intravenous irinotecan for patients with platinum-resistant and taxane-pretreated ovarian, tubal and peritoneal cancer as the test arm regimen in a subsequent Phase III trial.

Study Setting

The study is a multi-institutional open-label two-stage design Phase II trial.

Resources

This study is supported by Grants-in-Aid for Cancer Research (20S-1 and 20S-6) and Health and Labor Sciences Research Grant for Clinical Cancer Research (18–6), from The Ministry of Health, Labor and Welfare of Japan.

Endpoints

The primary endpoint is response rate in all eligible patients. For patients with measurable lesion, response is evaluated according to the RECIST criteria (19). For patients with non-measurable lesion, response is evaluated according to the GCIG CA-125 criteria (20). The secondary endpoints are progression-free survival, overall survival and adverse events. Overall survival is defined as days from registration to death from any cause, and it is censored at the last follow-up day when the patient is alive. Progression-free survival is defined as days from registration to disease progression (either of radiological, CA-125, symptomatic) or death from any cause, and it is censored at the latest day when the patient is alive without any evidence of progression.

Eligibility Criteria

Inclusion Criteria

For inclusion in the study, patients are required to fulfill all of the following criteria:

(i) cytologically or histologically proven ovarian, tubal or peritoneal cancer
(ii) platinum-resistant disease
(iii) taxane-pretreated disease
(iv) age: 20–75 years old
(v) PS (performance status): 0–2
(vi) one of the followings, or both of them:
  (a) patients have measurable lesion
  (b) patients have assessable lesion with elevated CA-125 (more than 70 U/ml)
(vii) no prior treatment with irinotecan, topotecan or etoposide
(viii) no prior radiation to abdomen
(ix) oral intake without parenteral nutrition
(x) both of the followings:
  (a) no drainage to effusion or ascites within 28 days
  (b) no effusion or ascites to be drained at registration
(xi) both of the followings:
  (a) no chemotherapy or surgery within 28 days
  (b) no hormonal or biologic therapy within 14 days
(xii) patients without severe organ dysfunction
(xiii) written informed consent

Exclusion Criteria

Patients are excluded if they meet any of the following criteria:

(i) synchronous or metachronous (within 5 years) malignance other than carcinoma *in situ* or intramucosal cancer
(ii) mental disease or mental symptoms that would affect the participant's decision to participate
(iii) pregnant or lactating
(iv) continuous systemic steroid

(v) active bacterial or fungal infection with fever of 38.5°C or higher
(vi) uncontrollable hypertension
(vii) uncontrollable diabetes requires continuous insulin administration
(viii) history of myocardial infarction or heart failure within 6 months, or current unstable angina
(ix) bowel obstruction

Treatment Methods

Etoposide is orally administered once a day at 50 mg/m^2 from days 1 to 21, and irinotecan is infused at 70 mg/m^2 on days 1 and 15, repeated every 28 days. Protocol treatment is continued up to six cycles unless disease progression, unacceptable toxicity or patient refusal.

Follow-up

Enhanced abdominal computed tomography (CT)/magnetic resonance imaging, chest CT/X-rays and tumor marker (CA-125) are evaluated at least every 8 weeks during the protocol treatment. Adverse events are evaluated at least every 2 weeks during the protocol treatment using CTCAE ver. 3.0.

Study Design and Statistical Analysis

This study is a Phase II trial with two-stage design by Southwest Oncology Group (21) to evaluate this regimen as the test arm for a subsequent Phase III trial.

The sample size was determined as follows by the SWOG design. We assumed that the expected value for the primary endpoint of 35% and the threshold value of 20%. In this situation, the sample size ensuring at least 80% power with one-sided α of 5% is 55. Considering the likelihood of some ineligible patients being enrolled, the total number of patients was set at 60.

Interim Analysis and Monitoring

We plan interim analysis for futility after 30 patients enrolled. In house monitoring will be performed every 6 months by the JCOG Data Center to evaluate the study progress and to improve the study quality.

PARTICIPATING INSTITUTIONS

The participating institutions (from north to south) are as follows: Hokkaido University Hospital, Sapporo Medical University, Iwate Medical University, Tohoku University Hospital, Institute of Clinical Medicine, Tsukuba University, National Defense Medical College, Saitama Cancer Center, Saitama Medical Center, Saitama Medical School, National Cancer Center Hospital, Jikei Kashiwa Hospital, Tokyo Metropolitan and Infectious diseases Center Komagome Hospital, The University of Tokyo Hospital, Jikei University Hospital, Cancer Institute Hospital, Juntendo University School of Medicine, Kitasato University School of Medicine, Niigata Cancer Center Hospital, Shinshu University School of Medicine, Aichi Cancer Center Hospital, Kyoto University Hospital, Osaka city University Hospital, Kinki University School of Medicine, Osaka Medical Center for Cancer and Cardiovascular Disease, Osaka City General Hospital, Sakai Hospital, Kinki University School of Medicine, Hyogo Cancer Center, Tottori University, Kure Medical Center Chugoku Cancer Center, Shikoku Cancer Center, Kyushu Cancer Center, Kurume University School of Medicine, Kyushu University Hospital, Faculty of Medicine Saga University, Kumamoto University Medical School, Kagoshima City Hospital and University of the Ryukyu.

Funding

This study is supported by National Cancer Center Research and Development Fund 23-A-17.

Conflict of interest statement

None declared.

References

1. Ozols RF, Bundy BN, Greer BE, Fowler JM, Clarke-Pearson D, Burger RA, et al. Phase III trial of carboplatin and paclitaxel compared with cisplatin and paclitaxel in patients with optimally resected stage III ovarian cancer: a Gynecologic Oncology Group study. *J Clin Oncol* 2003;21:3194–200.
2. Katsumata N, Yasuda M, Takahashi F, Isonishi S, Jobo T, Aoki D, et al. Dose-dense paclitaxel once a week in combination with carboplatin every 3 weeks for advanced ovarian cancer: a phase 3, open-label, randomised controlled trial. *Lancet* 2009;374:1331–8.
3. Gordon AN, Fleagle JT, Guthrie D, Parkin DE, Gore ME, Lacave AJ. Recurrent epithelial ovarian carcinoma: a randomized phase III study of pegylated liposomal doxorubicin versus topotecan. *J Clin Oncol* 2001;19:3312–22.
4. Mutch DG, Orlando M, Goss T, Teneriello MG, Gordon AN, McMeekin SD, et al. Randomized phase III trial of gemcitabine compared with pegylated liposomal doxorubicin in patients with platinum-resistant ovarian cancer. *J Clin Oncol* 2007;25:2811–8.
5. Vasey PA, Kaye SB. Combined inhibition of topoisomerases I and II–is this a worthwhile/feasible strategy? *Br J Cancer* 1997;76:1395–7.
6. Bodurka DC, Levenback C, Wolf JK, Gano J, Wharton JT, Kavanagh JJ, et al. Phase II trial of irinotecan in patients with metastatic epithelial ovarian cancer or peritoneal cancer. *J Clin Oncol* 2003;21:291–7.
7. Matsumoto K, Katsumata N, Yamanaka Y, Yonemori K, Kohno T, Shimizu C, et al. The safety and efficacy of the weekly dosing of irinotecan for platinum- and taxanes-resistant epithelial ovarian cancer. *Gynecol Oncol* 2006;100:412–6.
8. Takeuchi S, Dobashi K, Fujimoto S, Tanaka K, Suzuki M, Terashima Y, et al. A late phase II study of CPT-11 on uterine cervical cancer and ovarian cancer. Research Groups of CPT-11 in Gynecologic Cancers. *Gan To Kagaku Ryoho* 1991;18:1681–9.
9. Hainsworth JD, Greco FA. Etoposide: twenty years later. *Ann Oncol* 1995;6:325–41.

10. Maskens AP, Armand JP, Lacave AJ, De Jager RL, Hansen HH, Wolff JP. Phase II clinical trial of VP-16-213 in ovarian cancer. *Cancer Treat Rep* 1981;65:329–30.
11. Eckhardt S, Hernadi Z, Thurzo L, Telekes A, Sopkova B, Mechl Z, et al. Phase II clinical evaluation of etoposide (VP-16–213, Vepesid) as a second-line treatment in ovarian cancer. Results of the South-East European Oncology Group (SEEOG) Study. *Oncology* 1990;47:289–95.
12. Rose PG, Blessing JA, Mayer AR, Homesley HD. Prolonged oral etoposide as second-line therapy for platinum-resistant and platinum-sensitive ovarian carcinoma: a Gynecologic Oncology Group study. *J Clin Oncol* 1998;16:405–10.
13. Kim R, Hirabayashi N, Nishiyama M, Jinushi K, Toge T, Okada K. Experimental studies on biochemical modulation targeting topoisomerase I and II in human tumor xenografts in nude mice. *Int J Cancer* 1992;50:760–6.
14. Masumoto N, Nakano S, Esaki T, Tatsumoto T, Fujishima H, Baba E, et al. Sequence-dependent modulation of anticancer drug activities by 7-ethyl-10-hydroxycamptothecin in an HST-1 human squamous carcinoma cell line. *Anticancer Res* 1995;15:405–9.
15. Eder JP, Chan V, Wong J, Wong YW, Ara G, Northey D, et al. Sequence effect of irinotecan (CPT-11) and topoisomerase II inhibitors in vivo. *Cancer Chemother Pharmacol* 1998;42:327–35.
16. Gronlund B, Engelholm SA, Horvath G, Maenpaa J, Ridderheim M. Sequential topotecan and oral etoposide in recurrent ovarian carcinoma pretreated with platinum-taxane. Results from a multicenter phase I/II study. *Cancer* 2005;103:1388–96.
17. Yamanaka Y., Katsumata N., Watanabe T., Andoh M., Mukai H., Kitagawa R, et al. A dose finding study of irinotecan in combination with oral etoposide in patients with platinum treated advanced epitherial ovarian cancer. *Proc Am Soc Clin Oncol* 2002;21 (abstr 2521).
18. Nishio S, Sugiyama T, Shouji T, Yoshizaki A, Kitagawa R, Ushijima K, et al. Pilot study evaluating the efficacy and toxicity of irinotecan plus oral etoposide for platinum- and taxane-resistant epithelial ovarian cancer. *Gynecol Oncol* 2007;106:342–7.
19. Therasse P, Arbuck SG, Eisenhauer EA, Wanders J, Kaplan RS, Rubinstein L, et al. New guidelines to evaluate the response to treatment in solid tumors. European Organization for Research and Treatment of Cancer, National Cancer Institute of the United States, National Cancer Institute of Canada. *J Natl Cancer Inst* 2000;92:205–16.
20. Rustin GJ, Quinn M, Thigpen T, du Bois A, Pujade-Lauraine E, Jakobsen A, et al. Re: New guidelines to evaluate the response to treatment in solid tumors (ovarian cancer). *J Natl Cancer Inst* 2004;96:487–8.
21. Green SJ, Dahlberg S. Planned versus attained design in phase II clinical trials. *Stat Med* 1992;11:853–62.

IJC
International Journal of Cancer

Hypoxia upregulates ovarian cancer invasiveness *via* the binding of HIF-1α to a hypoxia-induced, methylation-free hypoxia response element of S100A4 gene

Akiko Horiuchi[1], Takuma Hayashi[2], Norihiko Kikuchi[1], Akiko Hayashi[1], Chiho Fuseya[1], Tanri Shiozawa[1] and Ikuo Konishi[3]

[1] Department of Obstetrics and Gynecology, Shinshu University Graduate School of Medicine, Matsumoto, Japan
[2] Department of Immunology and Infectious Disease, Shinshu University Graduate School of Medicine, Matsumoto, Japan
[3] Department of Gynecology and Obstetrics, Kyoto University Graduate School of Medicine, Kyoto, Japan

Hypoxia is known to play important roles in the development and progression of tumors. We previously demonstrated that S100A4, a critical molecule for metastasis, was upregulated in ovarian cancer cells. Therefore, we examined the mechanisms of the upregulation of S100A4 expression in ovarian carcinoma cells, with particular attention paid to the effects of hypoxia. The expression levels of S100A4 were found to be correlated with the invasiveness of ovarian carcinoma cells *in vitro* and *in vivo*, and the upregulation of S100A4 expression was associated with hypomethylation of CpG sites in the first intron of S100A4 in ovarian carcinoma cell lines and tissues. The expression of S100A4 was increased under hypoxia and was associated with elevated invasiveness, which was inhibited by S100A4 small interfering RNA (siRNA). In addition, exposure to hypoxia reduced the methylation of hypoxia-response elements (HRE) of the S100A4 gene in a time-dependent fashion, in association with the increased binding of HIF-1α to a methylation-free HRE in ovarian carcinoma cells. These results indicate that hypoxia-induced hypomethylation plays an essential role in S100A4 overexpression and the epigenetic transformation of ovarian carcinoma cells into the "metastatic phenotype."

The metastatic potential of tumor cells has been reported to be regulated by their interactions with their microenvironment. These interactions can be modified by the accumulation of genetic and epigenetic changes, which are transient alterations induced by the local tumor microenvironment. In particular, the role of microenvironmental hypoxia has been focused on with regard to tumorigenesis, tumor progression and tumor biology.[1–4] Hypoxia is known to induce the expression of the transcription factor hypoxia-inducible factor (HIF), which has been reported to be upregulated in human malignancy.[5] HIF binds to hypoxia-response elements (HRE)[3] and activates the transcription of various target genes, not only angiogenetic factors but also metastasis-associated genes.[6] We previously reported that hypoxia was associated with invasive phenotypes in ovarian carcinomas.[7,8]

Key words: S100A4, hypoxia, hypomethylation, ovarian carcinoma
Additional Supporting Information may be found in the online version of this article.
Grant sponsor: Ministry of Education, Science and Culture of Japan (Grants-in-Aid for Scientific Research); **Grant numbers:** 1859182, 20591942, 19390426
DOI: 10.1002/ijc.27448
History: Received 22 Jul 2011; Accepted 2 Jan 2012; Online 27 Jan 2012
Correspondence to: Akiko Horiuchi, Department of Obstetrics and Gynecology, Shinshu University School of Medicine, 3-1-1 Asahi, Matsumoto 390-8621, Japan, Tel.: +81-263-37-2718, Fax: +81-263-34-0944, E-mail: aki9hori@shinshu-u.ac.jp

In addition, HIF-1α overexpression is associated with a poor prognosis in patients with ovarian cancer,[9] suggesting that hypoxia is important for the acquisition of aggressive behavior in ovarian cancer cells.

S100A4, which is also known as mts-l/metastasin/pEL98/p9k,[10,11] belongs to the calcium binding S100 protein family. Altered expression levels of S100 proteins have been reported in several human diseases, such as cancer, inflammatory disorders and neurodegenerative conditions and are associated with cell motility and invasion.[11] Interestingly, a recent report suggested that cancer cells induce S100 expression to produce an appropriate metastatic site *via* an autocrine/paracrine pathway[12,13] and that S100A4 might be a cancer stem cell (CSC) marker.[14] We also reported that S100A4 expression was upregulated in ovarian cancer and that the expression of S100A4 was an independent prognostic factor in patients with ovarian cancer.[15] However, little is known about the mechanism of the altered expression of S100A4 in ovarian carcinomas.

One of the mechanisms of S100A4 upregulation was reported to be the hypomethylation of CpG sites in the first intron of the S100A4 gene in human carcinoma cell lines.[16–20] Epigenetic changes were found to occur in various target genes during cancer development and progression.[21] Although the hypermethylation of tumor-suppressor genes has been studied in detail, genome-wide hypomethylation has also been reported in various human cancers.[22,23] Functionally, hypomethylation affects the expression of selected genes such as MAGE, γ-synuclein, S100A4 and others.[24–26] In addition, the

expression of S100A4 was suggested to be induced by hypoxia in mouse pulmonary arteries.[27] However, the mechanisms of hypoxia-induced S100A4 upregulation are not fully understood. Therefore, we hypothesized that the increased S100A4 expression observed during hypoxia might be associated with local epigenetic alterations. To address this issue, we examined the expression of S100A and epigenetic changes in ovarian cancer cells under hypoxia.

Material and Methods

Cell culture

The ovarian cancer cell lines SKOV3 and OVCAR3 were purchased from the ATCC (Rockville, MD). The ovarian cancer cell lines A2780 and A2780/CDDP (a cisplatin-resistant cell line derived from A2780) were kind gifts from Dr. Takashi Tsuruo (Cancer Chemotherapy Center, Tokyo, Japan) with the permission of Dr. Thomas C. Hamilton (Fox Chase Cancer Institute, Philadelphia, PA).[28]

Normal ovarian surface epithelial (OSE) cells. The immortalized ovarian surface cell line OSE2a was provided by Dr. Hidetaka Katabuchi (Kumamono University, Kumamoto, Japan).[29] Incubation was carried out at 37°C under 20% O_2 for normoxia or at 37°C under 1% O_2 for hypoxia.

Cell treatments

The cells were cultured in medium containing 1 μM 5-aza-deoxycytidine (5Aza-dC; Sigma-Aldrich, St. Louis, MO) for 96 hr or 1 μM trichostatin A (Sigma-Aldrich) for 24 hr. On the third day of treatment, the media were replaced with fresh media containing 5-azadC.

Plasmid construction

Human genomic DNA was extracted from A2780 cells and used to amplify the S100A4 promoter and intron1 from position −4 to +997 relative to the transcription start site by polymerase chain reaction (PCR). Sequence data were analyzed using the Basic Local Alignment Search Tool (BLAST) on the National Center for Biotechnology Information website (http://www.ncbi.nlm.nih.gov). F −4: 5′-ggggtacccccccattc ttcccctctctacaaccctctctcctcagcg-3′, F +248: 5′-ggggtaccaacag aaaagtgagcaagtgactgaatttgagctctccaggtg-3′, F +383: 5-gggg taccttgcgcactcgggagcaggaagcaaaggaaaggcagaagg-3′, F +718: 5′-ggggtaccgctgttgttgaggaaggcctgg gaggccctgggagtttg-3′ and R: 5′-aacacatctctgaggggtggaagcttcg-3′. These products were digested with Kpn I and Hind III and ligated into -pGL3.10-Luc (pLuc3) (Promega, Madison, WI) and renamed pLuc3(-4), pLuc3(248), pLuc3(383) and pLuc3(718), respectively. All constructs were sequenced in a capillary automatic sequencer (ABI PRISM 3100 Genetic Analyzer, Applied Biosystems) and matched to the published human S100A4 sequence.

Reporter constructs including point mutations at potential HIF1 binding sites, HRE1 and HRE2 in S100A4 intron 1 were constructed using the site-directed mutagenesis system according to the manufacturer's protocol (Promega). The DNA sequence of mutagenic oligonucleotides for mutant HRE1 and HRE2 were as follows: mutant HRE1 5′-CTCTGG GTGGATTGTGTgaaagGGTGTGCATGGCACACAC-3′ and mutant HRE2 5′-CGCTGTTGCTATAGTaaaagTTGGTATGT ATGTGCCTGTGGG-3′.

Luciferase reporter analysis

Transfection was performed on the day the cell layer reached 50–60% confluence using the Effectene Transfection Reagent (Qiagen, Valencia, CA, according to the manufacturer's protocol. Two days after transfection, luciferase activity was assayed using the Steady Glo or Bright Glo luciferase assay reagent and dual luciferase reporter assay reagents (Promega). All experiments were repeated at least three times. To induce methylation, pLuc3(-4) was treated with s-adenosyl-[methyl-3H] methionine (SAM; Amersham LIFE SCIENCE, Amersham Place, Little Chalfont, Buckinghamshire HP7 9NA, England), which is the principle biological methyl donor, and was then transiently transfected into A2780/CDDP.

Small interfering RNA (siRNA) transfection

siRNA oligonucleotides targeting HIF-1α (target sequence: 5′-AAAGGACAAGUCACCACAGGA-3′) were obtained from Qiagen (Valencia, CA). The siRNA for S100A4 (5′-AGCUU-GAACUUGUCACCCTC-3′) and the silencer-negative siRNA for the control were purchased from Ambion (Austin, TX). The sequences for the S100A4 siRNAs used are available on request. The cultured cells were then transfected with the corresponding siRNA using Oligofectamine (Invitrogen, Carlsbad, CA) according to the manufacturer's protocol.

Chromatin immunoprecipitation assay

The ChIP-IT kit was purchased from ActiveMotif (Carlsbad, CA), and the ChIP assay was carried out according to the manufacturer's protocol. One microgram of rabbit polyclonal antibody to HIF-1α or Sp1 (Santa Cruz Biotechnology, Santa Cruz, CA) was utilized for immunoprecipitation. After proteinase K digestion and DNA precipitation, 3 μl of diluted DNA were used for PCR. The primer sequences were as follows: HRE1 forward 5′-agttgtgttggcctgactgg-3′, HRE1 reverse 5′-aag cacctggagagagctcaaat-3′; HRE2 forward 5′-tgcatggcacacacacacat -3′, HRE2 reverse 5′-ttagctctcagcatgggga-3′; Sp1BS forward 5′-ctgcagcttctcttccaacc-3′, Sp1BS reverse 5′-tttttccacccctcactcactcag-3′. Following 28 cycles of amplification, the PCR products were run on a 3.0% agarose gel and analyzed by ethidium bromide staining. The band intensity was measured and normalized to the results for the input control samples.

Immunofluorescence staining of S100A4

Ovarian cancer cells were grown on a four-well Lab-Tek Chamber Slide for 24 hr before the hypoxia treatment. Cells were then transferred to hypoxia (1% O_2) or let in normoxia. For hypoxia experiments, 150 μm of pimonidazole (Hypoxyprobe, Burlington, MA) was added to the medium for 2 hr. After washing with phosphate buffered saline (PBS), cells

were fixed with paraformaldehyde (3%) for 10 min at room temperature and subsequently washed again with PBS. After blocking with bovine serum albumin, slides were incubated for 12 hr with anti-S100A4 rabbit antibody (Santa Cruz Biotechnology, Santa Cruz, CA) and anti-Hypoxyprobe(tm)-1 mouse monoclonal antibody 1 (mAb1, 1:100 dilution) from the Hypoxyprobe(tm)-1 Plus kit (Hypoxyprobe). Then, the slides were washed with PBS and incubated with the Alexa fluor 546-labeled anti-rabbit IgG and Alexa fluor 488-labeled anti-mouse IgG1 as secondary antibodies at room temperature for 3 hr. Nuclei were counterstained with VECTASHIELD mounting medium with 4′,6-diamidine-2′-phenylindole dihydrochloride (DAPI, 1.5 μg/ml) (Vector Laboratories, Burlingame, CA) according to the manufacturer's instructions. All specimens were examined using confocal laser scanning microscopy (Leica TCS SP2; Leica Microsystems, Wetzlar, Germany).

Immunofluorescence staining of 5-methyl-cytosine

Cultured Cells were fixed in cold acetone for 15 min. Then, the cells were incubated with RNase A (50 μg/ml) for 1 hr at 37°C and washed with PBS. To denature DNA, the samples were incubated in 0.3M HCl for 30 min at 37°C. After denaturation, the samples were blocked with 0.4% BSA overnight at 4°C and then incubated with mouse anti-5-methyl-cytosine (5-mC) primary antibody (Calbiochem, 1:1,000) for 3 hr at 37°C. This was followed by anti-mouse fluorescein-5-isothiocyanate (FITC) secondary antibody incubation (1:200) (Sigma-Aldrich) for 1 hr at RT. Nuclei were counterstained with VECTASHIELD mounting medium with DAPI (Vector Laboratories). The control slides received PBS in place of the primary antibody. The immunostained cells were counted in a blinded fashion.

Western blot analysis

Extracts equivalent to 50 μg of total protein were separated by sodium dodecyl sulfate (SDS)-polyacrylamide gel electrophoresis and transferred onto nitrocellulose membranes, as described previously.[30,31] Primary antibodies against S100A4 (Santa Cruz Biotechnology) or β-actin (Sigma-Aldrich) were used. The densities of the bands on the filters were quantified by densitometric analysis using the Quantity One Scan System (ATTO, Tokyo, Japan).

Reverse transcription polymerase chain reaction (RT-PCR)

RT-PCR was performed using an RNA PCR Kit (Takara Shuzo, Otsu, Japan), as described previously.[15,31,32] Primers encompassing specific segments of the cDNA sequence of the S100A4 (sense, 5′-agcttcttggggaaaaggac-3′ and antisense, 5′-ccccaaccacatcagagg-3′) and glyceraldehyde-3-phosphate dehydrogenase (GAPDH) (sense, 5′-acgaccactttgtcaagctc-3′ and antisense, 5′-ggtctacatggcaactgtga-3′) genes were synthesized. After 35 cycles of amplification, the PCR products were analyzed, and the bands were visualized using ethidium bromide.

Real-time RT-PCR

To confirm the results of RT-PCR, mRNA expression was also analyzed using real-time PCR (LightCycler, Roche, Mannheim, Germany) as described previously.[30]

In vitro invasion assay

Cell invasion through a reconstituted basement membrane, Matrigel (Becton Dickinson Labware, Bedford, MA), was assayed according to a previously reported method.[7,32] After 16 hr of incubation, the cells on the upper surface of the filter were removed carefully with a cotton swab, the membranes were stained with Diff-Quik solution (Kokusai-Shiyaku, Kobe, Japan), and cells that had migrated through the membrane to the lower surface were counted in ten different fields under a light microscope at ×100 magnification. Each experiment was performed in triplicate wells and repeated three times.

Nude mice tumorigenicity assay

Three ovarian cancer cell lines were trypsinized and then resuspended in Dulbecco's modified eagle medium (DMEM) and 5% fetal calf serum (FCS) at a concentration of 1×10^7/ml. Six-week-old nude mice (BALB/c Slc-nu; Japan SLC, Hamamatsu, Japan) were injected with 5×10^6 cells in the abdominal cavity. The care and use of these experimental animals was in accordance with institutional guidelines. The mice were observed weekly and sacrificed after 1 month. Individual disseminated tumors were counted and evaluated by the percentage of tumor development among injected mice, described as the dissemination rate.

Case selection and DNA preparation

A total of 61 primary epithelial ovarian cancers were subjected to immunohistochemical analysis. Sixty-one consecutive patients with ovarian carcinoma visited Shinshu University Hospital between 1994 and 2003 and underwent surgery followed by cisplatin-based chemotherapy. The follow-up period ranged from 3 to 160 months (median: 76 months). According to the International Federation of Gynecology and Obstetrics (FIGO) classification, 33 carcinomas were classified as Stage I, 10 were classified as Stage II, 21 were classified as Stage III and five were classified as Stage IV. Histologically, 25 were serous, five were mucinous, 22 were clear cell and 17 were endometrioid adenocarcinomas. Each tissue sample was used with the approval of the Ethics Committee of Shinshu University School of Medicine.

For DNA preparation, 52 epithelial ovarian tumors were available. Sections were deparaffinized, rehydrated and dried. To extract DNA, the fields of interest were selected and microdissected, as described previously.[9,33]

DNA methylation analysis using sodium bisulfite sequencing

Five hundred nanograms to 1 μg of genomic DNA were modified with sodium bisulfite. The DNA was then treated

with the CpGenome DNA Modification Kit according to the manufacturer's recommendations (Intergene, NY), and the modified DNA was used for PCR together with primers based on the GenBank sequence NM_000264. Primer sequences were MSP-1F: GTTTGGTGGTGTGTTTTATGAGTTTTTG, MSP-1R: CCCCTCAAAAATATATTCAAAATACCAAACTCCAC, MSP-2F: GAAGGTAATTGTGGGTTTTTGT and MSP-2R: ACCTTACCTCAACAACAACATTT. The methylation statuses of 11 CpG siteswithin a 585-bp amplicon spanning the S100A4 first intron were evaluated. PCR was performed for 45 cycles using HotStar™ *Taq* DNA polymerase (Qiagen, Hilden, Germany), and the amplified products were purified using a QIAquick PCR purification kit (Qiagen) and then cycle sequenced in both directions with the DYEnamic ET Terminator Kit (Amersham). The resultant sequence was analyzed in a capillary automatic sequencer (ABI PRISM 3100 Genetic Analyzer). At least three PCR products for each sample were sequenced by standard methods. The results of sodium bisulfite sequencing were scored according to the method of a previous report.[34] The ratio of cytosine (methylated) to thymidine (unmethylated) at each CpG site was graded as follows: white, hypomethylation (the peak height of the methylated signal was lower than 0.5 relative to the unmethylated signal); gray, hemimethylation (the peak height of the methylated signal was between 0.5 and 1.5 relative to the unmethylated signal); black, methylation (the peak height of the methylated signal was higher than 1.5 relative to the unmethylated signal). The hypomethylation rate was evaluated as the percentage of hypomethylated CpG sites.

Immunohistochemical analysis

Immunohistochemical staining was performed on serial paraffin-embedded sections. For S100A immunostaining, the strept-avidin-biotin-peroxidase complex method (Histofine MAX-PO kit, Nichirei, Tokyo, Japan) was used, as described previously.[15] Immunoreactive tumor cells were semiquantitatively estimated by comparing them with a positive internal control; *i.e.*, lymphocytes and vascular smooth muscle cells that demonstrated positivity for S100A4 in their cytoplasm. Cytoplasmic staining was classified as: (−) negative, 0–10% positive cells; (+) weakly positive, 10–50% positive cells; (++) strongly positive, more than 50% positive cells.[15] Nuclear staining was defined as follows: (−) negative, 0–20% positive cells; (+) positive, more than 20% positive cells.

The Catalyzed Signal Amplification System (DAKO, Carpinteria, CA) was used for HIF-1α immunostaining, as described previously.[7,9] The primary antibody, mouse anti-HIF-1α monoclonal antibody (Novus Biologicals, Littleton, CO), was used at a dilution of 1:1,000. The cases were classified as positive (>5% of tumor cells with nuclear staining) or negative (<5% of tumor cells with nuclear staining).[9] The evaluation of immunostaining was performed by two independent observers (N.K. and A.H.) who were unaware of the fate of the patient or the tissue site.

Enzyme assay for DNA methyltransferase

Total protein was extracted using the EpiQuik Nuclear Extraction Kit (Epigentek, NY). The Bradford protein assay was used to determine protein concentrations, and the same amount of protein was measured in each sample using the EpiQuik DNA Methyltransferase Activity/Inhibition Assay (Epigentek), which was performed according to the manufacturer's instructions. The values were normalized to the background absorbance of the culture medium alone.

Statistical analyses

Values represent the mean ± SD. Fischer's exact test, Student's *t*-test, the Kruskal-Wallis test and Mann-Whitney's U-test were used to assess the significance of differences. Spearman's rank correlation was used to determine whether there was a positive or negative correlation among HIF-1α and S100A4 expression. The log-rank test was used to evaluate significant predictors of survival. Cumulative survival was also analyzed using the Kaplan-Meier method. Differences were considered significant when $p < 0.05$. These analyses were performed using SPSS Version 14 (SPSS, Chicago, Illinois).

Results

S100A4 is expressed in ovarian carcinoma cells and is localized in the cytoplasm or nucleus

We examined S100A4 expression and its functional relevance to intracellular localization and invasiveness in ovarian carcinoma cell lines. Immunofluorescent staining of S100A4 showed diffuse staining in both the cytoplasm and nucleus in A2780/CDDP cells. In SKOV3 cells, diffuse staining of S100A4 was observed in the cytoplasm. In OVCAR3 and OSE2a cells, the expression of S100A4 was faint (Fig. 1*a*). Western blot analysis of the cytoplasmic and nuclear fractions confirmed the subcellular expression pattern of S100A4 in 4 ovarian carcinoma cell lines (Fig. 1*b*). The Matrigel invasion assay showed that the invasive activity of A2780/CDDP cells, which express S100A4 in their nuclei, was significantly higher than those of the SKOV3 and OVCAR3 cells (Fig. 1*c*). To confirm the role of S100A4 in invasiveness, we transfected S100A4 specific siRNA into A2780/CDDP cells and found that the silencing of S100A4 expression resulted in decreased invasiveness (Fig. 1*d*). We then examined the tumor formation rate after the intraperitoneal injection of these cells into nude mice. The dissemination rate was 10/12 (83%) for A2780/CDDP cells, 3/11 (27%) for SKOV3 cells and 1/11 (9%) for OVCAR3 cells (Fig. 1*e*). Accordingly, the *in vivo* disseminated metastatic activity was correlated with S100A4 expression in the three cell lines.

S100A4 expression is related to the methylation status of S100A4 in ovarian cancer cells

It has been reported that the first intron of the S100A4 gene is important for S100A4 expression.[16–18] A luciferase assay

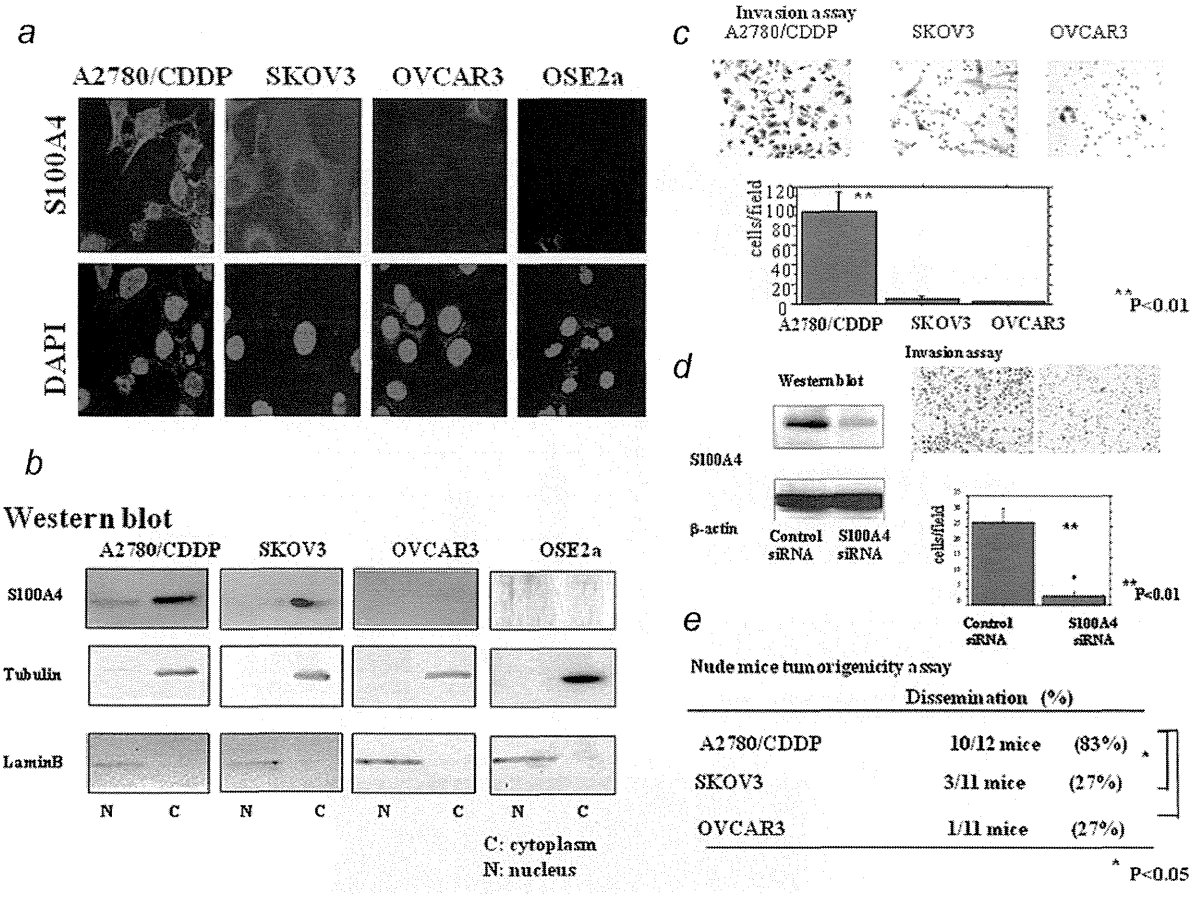

Figure 1. (*a*) Immunofluorescent analysis of S100A4 in ovarian carcinoma cell lines. Immunofluorescent staining of S100A4 showed diffuse staining in both the cytoplasm and nucleus in A2780/CDDP cells. In SKOV3 cells, diffuse staining of S100A4 was observed in the cytoplasm. In OVCAR3 and OSE2a cells, the expression of S100A4 was faint. Upper panel: S100A4 staining (red), Lower panel: Nuclei were counterstained with DAPI (blue). (*b*) Western blot analysis of the cytoplasmic and nuclear fractions. This analysis confirmed the subcellular expression pattern of S100A4 in 4 ovarian carcinoma cell lines. N: nuclear fraction and C: cytoplasmic fraction. (*c*) Matrigel invasion assay. The number of cells that passed through Matrigel-coated membranes was used to represent invasive activity. The Matrigel invasion assay showed that the invasive activity of A2780/CDDP cells, which express S100A4 in their nuclei, was significantly higher than those of SKOV3 and OVCAR3 cells. $*p < 0.05$. Student's *t*-test. (*d*) Matrigel invasion assay after the transfection of S100A4 siRNA. To confirm the role of S100A4 in invasiveness, we transfected S100A4 specific siRNA into A2780/CDDP cells. The reduction in S100A4 expression caused decreased invasiveness. $*p < 0.05$. Student's *t*-test. (*e*) Nude mouse tumorigenicity assay. We examined the tumor formation rate at 1 month after the intraperitoneal injection of the cells into nude mice. The frequency of nude mouse dissemination was correlated with the expression level of S100A4 in ovarian cancer cell lines tested. Individual disseminated tumors were evaluated by the percentage of tumor development among injected mice, described as the dissemination rate. The frequency of nude mouse dissemination was correlated with the expression level of S100A4 in all ovarian cancer cell lines tested.$*p < 0.05$. Fischer's exact test.

showed that the transcriptional activity of the S100A4 first intron was similar to that of endogenous S100A4 expression (Supporting Information Fig. 1). This sequence has 11 CpG sites (Supporting Information Fig. 1). Therefore, we investigated the association between the methylation statuses of these 11 CpG sites and the expression of S100A4 in ovarian carcinoma cells. The examination of sodium bisulfite-modified DNA showed that the hypomethylation of the CpG sites in the first intron is correlated with increased S100A4 expression (Fig. 2*a*).

To confirm the effect of CpG methylation on S100A4 expression *in vitro*, OVCAR3 cells were continuously exposed to 5Aza-dC. The expression of S100A4 was increased at both the mRNA and protein levels after 5-Aza-dC treatment in a time-dependent manner (Fig. 2*b*). Real-time RT-PCR showed that the S100A4 expression of OSE2a, OVCAR3 and SKOV3

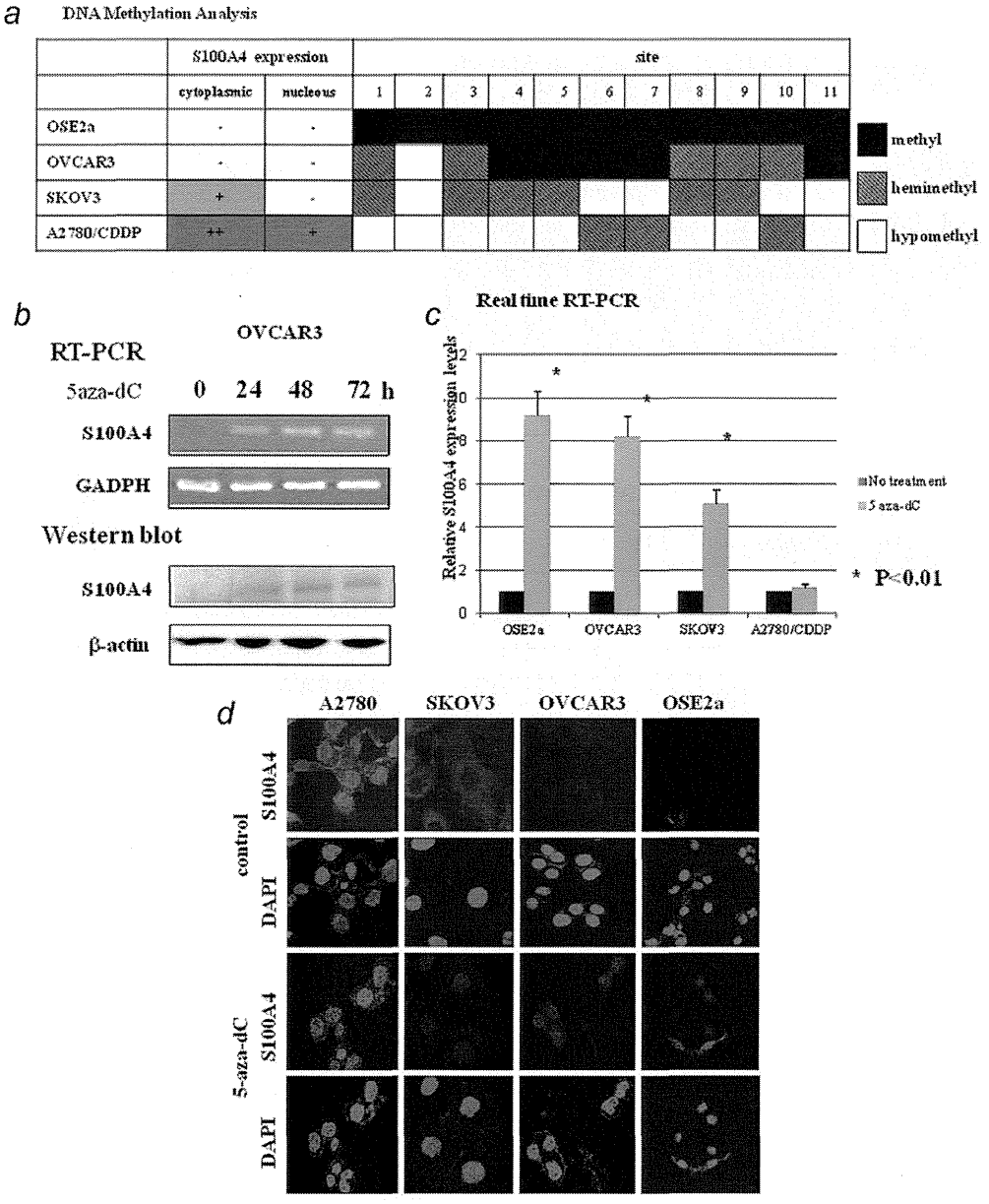

Figure 2. (*a*) DNA methylation analysis of S100A4 using sodium bisulfite sequencing. All 11 CpG sites of the first intron were methylated in OSE2a cells, which do not express S100A4. OVCAR3 cells showed very low endogenous expression of S100A4 mRNA and demonstrated that 10/11 sites were methylated or hemimethylated. A2780/CDDP cells, which have high endogenous levels of S100A4 mRNA, demonstrated that 8/11 sites were hypomethylated. The hypomethylation frequency was intermediate in SKOV3 cells. White: hypomethylated, gray: hemimethylated and black: methylated. (*b*) RT-PCR and Western blot analyses of the expression of S100A4 in OVCAR3 cells after 5-Aza-dC treatment. The expression of S100A4 was increased at both the mRNA and protein levels after 5-aza-dC treatment in a time-dependent manner. 5-aza-dC: 1 μM 5-aza-dC. (*c*) Changes in S100A4 mRNA expression after 5-Aza-dC treatment. The relative expression levels of S100A4 were estimated by real-time RT-PCR. The mRNA expression of S100A4 was increased after 5-aza-dC treatment in OSE2a, OVCAR3 and SKOV3. 5-aza-dC: 1 μM 5-aza-dC 96 hr, Values are the mean ± SD. *$p < 0.05$. Student's *t*-test. (*d*) Immunofluorescent analysis of S100A4 expression by treatment with 5-aza-dC. The changes of S100A4 localization after treatment with 5aza-dC were examined by immunofluorescence staining. 5-aza-dC treatment increased the nuclear expression of S100A4 in SKOV3, OVCAR3 and OSE2a. Upper panel: S100A4 staining (red), Lower panel: Nuclei were counterstained with DAPI (blue). 5-aza-dC: 1 μM 5-aza-dC for 96 hr.